MAGELLAN PROJECT

University of Arizona | Carnegie Institution of Washington | The Johns Hopkins University

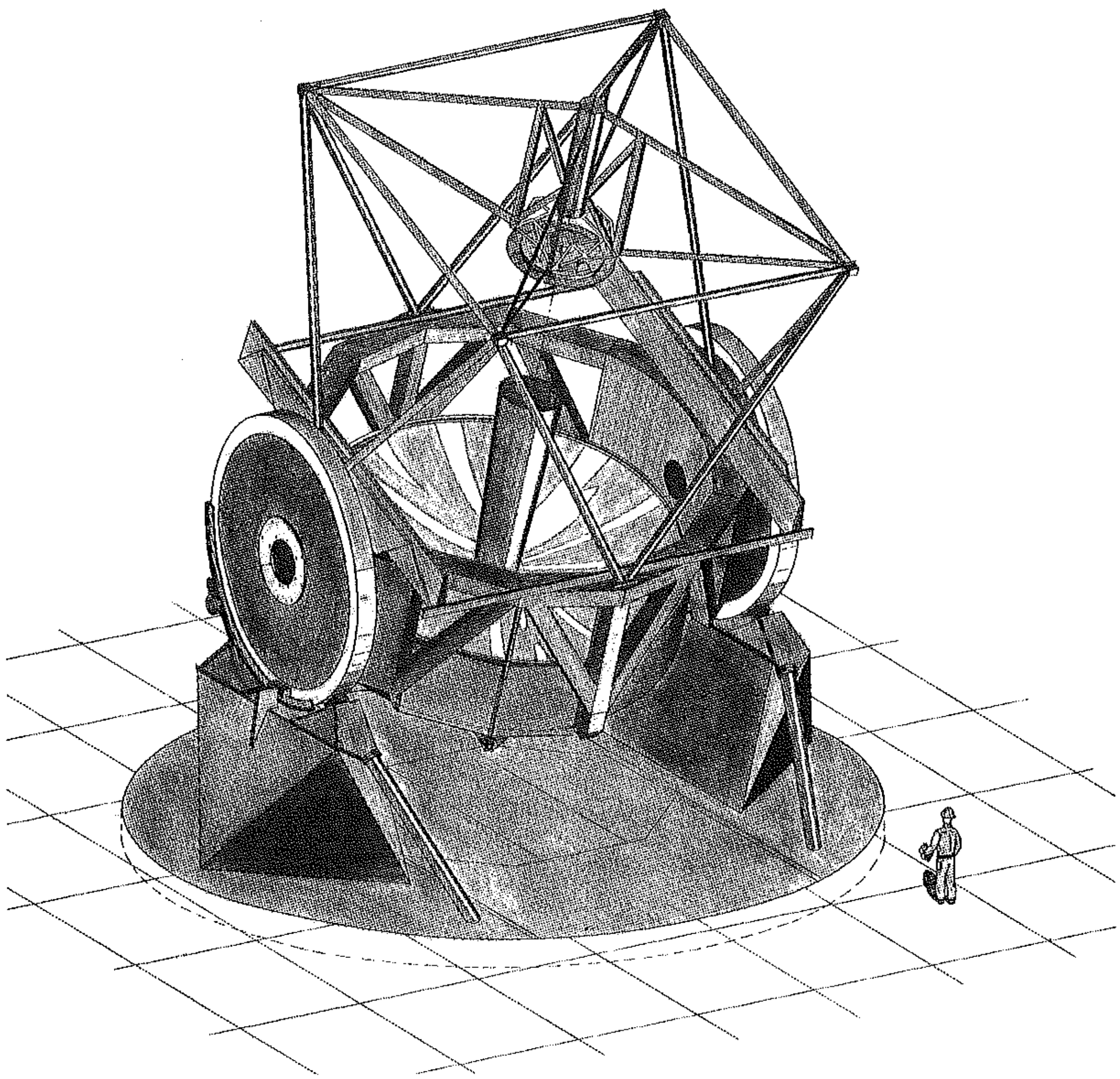

Boundary Conditions, Vibrational Modes, and Frequency Responses: What's Important for Telescope Performance?

J. Alan Schier
The Observatories of the
Carnegie Institution of Washington
Pasadena, California

February 1991
No. 29

INDEX

INTRODUCTION AND SUMMARY

This report examines a three-body mechanical system in order to determine how the natural modes of vibration enter into the system dynamics. The results outline the impact of the various modes on servo performance when applied to a practical telescope.

The analytical model used in this report represents a generic drive system with significant flexibilities in the driven load and in the driving "gearbox". Position measurement is made at the load, with torque at the motor as the controlled input. The system exhibits locked rotor, locked encoder, and free boundary modes of vibration when the corresponding boundary conditions are applied. Additionally, the frequency response between the input torque and the output position is derived.

Overall, the system's frequency response from input to output provides the best measure of both the obtainable servo crossover frequency and the disturbance rejection in the completed system.

The results indicate that the obtainable servo crossover frequency is most strongly affected by the compliance in the "gearbox", that is, the compliance between the point where the torque is applied and where the position measurement is made. This mode is capable of driving a servo system unstable. The importance of this mode is seen directly in the frequency response. The mode also appears in the free boundary modes of vibration.

The results also show low frequency modes which do not necessarily limit the servo crossover frequency, but which do however degrade disturbance rejection. Again, these modes show up directly in the frequency response. A bit more indirectly, the effect of these modes can be estimated from the locked encoder or free boundary modes.

The locked rotor modes are of no concern for the type of servo system considered in this report.

As a special warning, the results developed in this report do not apply to systems in which there is closed loop control around the drive motor position or velocity.

DESCRIPTION OF THE MODEL

Figure 1 shows the three-inertia, two-spring model used in this analysis. The two largest inertias simulate the first flexible mode of a telescope structure. The smallest inertia simulates the flexible mode that primarily involves the motor rotor and the drive compliance. The drive is assumed to have a gear ratio of N:1.

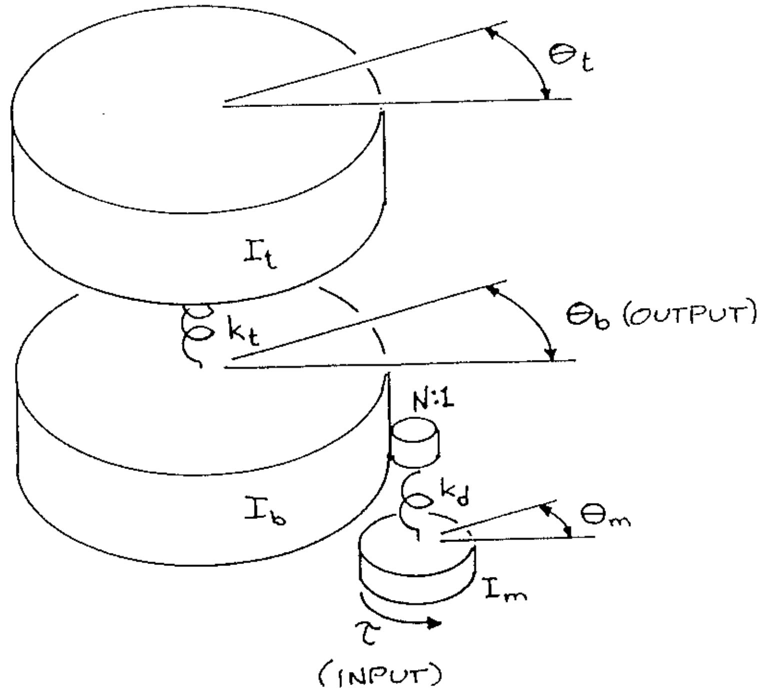

Figure 1: A three-body, two-spring model is used to simulate the first flexible mode of a telescope and the dominant drive compliance. A drive ratio of N:1 is included. For frequency response analysis, torque at I_m is the input variable, and the position of I_b is the output.

This analysis uses parameter values that could represent a large telescope such as the Magellan Project 8-m. The values are as follows.

<u>Model Parameters</u>

I_t	$2x10^6$	kg*m^2
I_b	$2x10^6$	kg*m^2
I_m	1	kg*m^2
k_t	$7.896x10^9$	N*m/rad
k_d	$2.467x10^6$	N*m/rad
N	40	

This model is analyzed to find the natural modes of vibration under the conditions of locked rotor (I_m grounded), locked encoder (I_b grounded), and free boundaries. Additionally, the input-output frequency response is derived.

RESULTS

Using the parameters above, the model exhibits the following frequencies of vibration.

Condition	First Mode	Second Mode
Locked rotor (I_m grounded)	0.1250 Hz	14.1427 Hz
Locked encoder (I_b grounded)	10.0 Hz	250.0 Hz
Free boundaries	14.1393 Hz	250.10 Hz

The calculation of these frequencies is given in Appendix B. The fact that several of the listed frequencies are very nearly but not quite equal is not a general result. This result is particular to this case and is due to I_m and k_d being orders of magnitude smaller than I_b and k_t.

Figure 2 shows the magnitude response for the same system with an input torque at I_m and output position taken at I_b. The frequencies of the features shown in Figure 2 are seen to be the same as some of the frequencies listed above. The calculation of the frequency response is given in Appendix A.

Referring to Figure 2 and going from low to high frequencies, the first feature is an antiresonance at 10 Hz and corresponds to the first locked encoder mode. The next feature is a resonance at 14.1393 Hz which corresponds to the first free boundary mode. The last feature is a resonance at 250.10 Hz, which is the second free boundary mode.

Figure 3 shows the phase response associated with this system, and there are two notable features in this plot. The first is the region of phase lead occurring just after 10 Hz, the frequency of the first antiresonance. The second is the transition to a large phase lag just after 250 Hz, the frequency of the second resonance.

For the type of system considered, the locked rotor mode frequencies only coincidentally resemble any of the other frequencies. The mode near 14 Hz is close to one of the free boundary frequencies because k_d is orders of magnitude smaller than k_t. In general, this similarity does not exist. The mode at 0.125 Hz is truly meaningless for the servo system and telescope performance since it does not enter into the servo frequency response.

IMPLICATIONS OF THE RESULTS

Perhaps the most significant result is that neither the locked rotor, locked encoder, or free boundary modes show all the features necessary for the accurate design and evaluation of a servo control system. Only the frequency response with the proper input and output (in this case torque and position of the load) gathers all the important features into one place and shows how they enter into the system behavior.

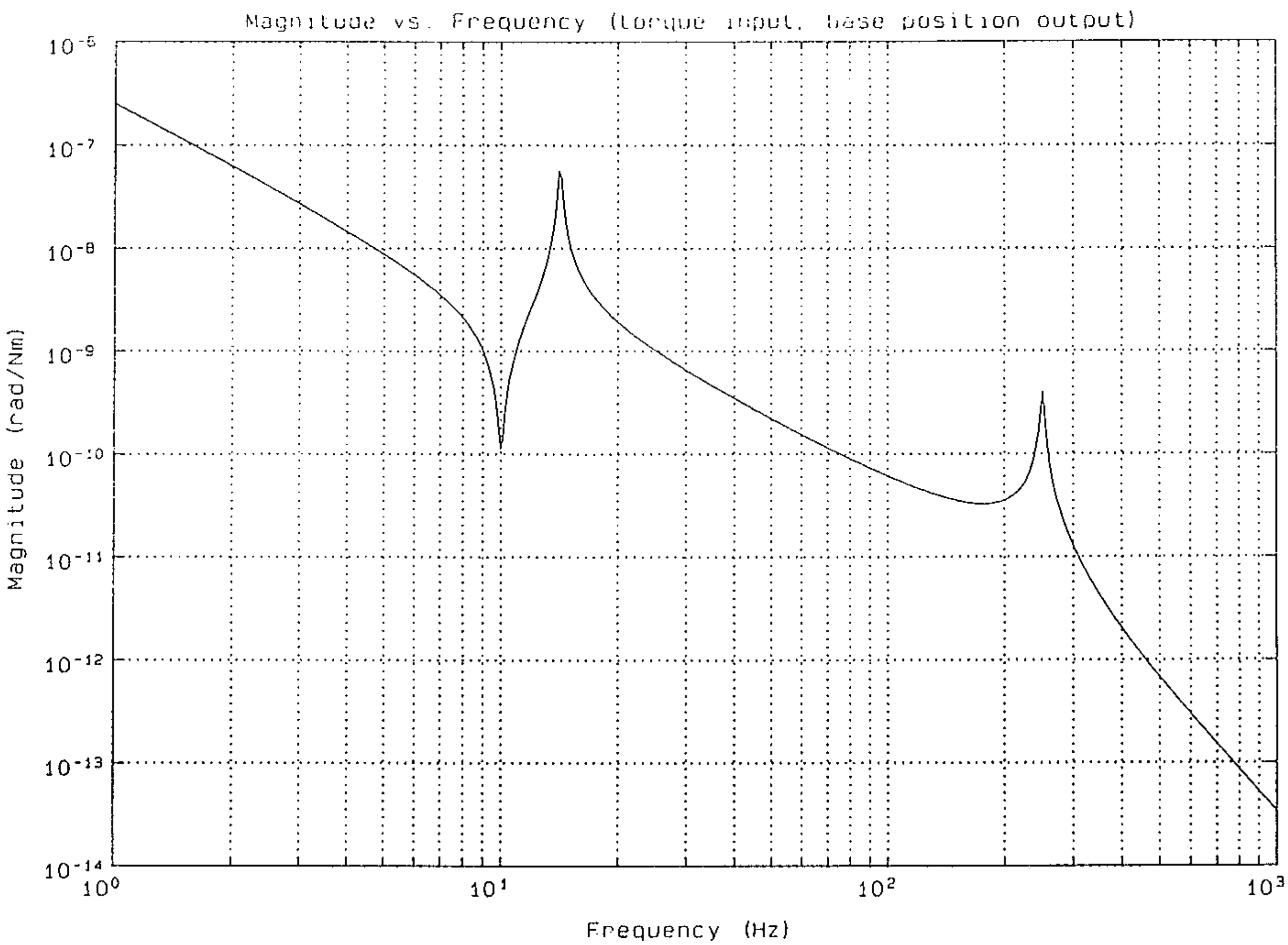

Figure 2: The magnitude response of the model system shows one antiresonance followed by two resonances. This response was calculated using the model parameters given in the text with a small amount of damping added to keep the peaks and valley finite.

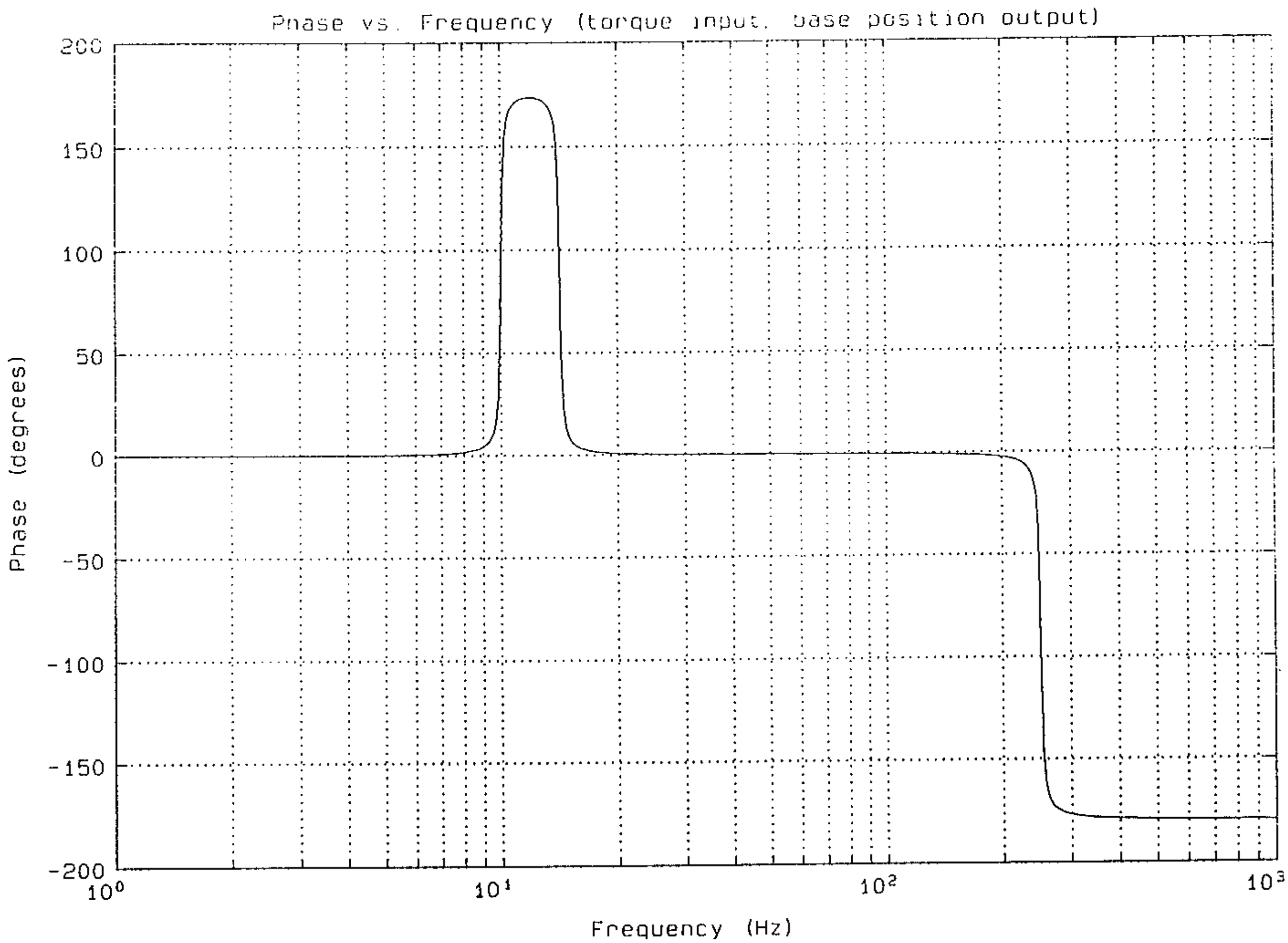

Figure 3: The phase response of the model system shows a small area of phase lead followed by a steep transition to negative phase angles. This response was calculated using the model parameters given in the text with a small amount of damping added. This plot has been shifted 180 degrees to remove the effect of the rigid body mode and center the plot around 0 degrees.

Referring to the magnitude and phase responses shown in Figures 2 and 3, the results indicate that the frequency of the third mode near 250 Hz is of notable importance. It is at this frequency that the phase makes a steep transition to large negative values. This phase lag combined with the sharp peak in the magnitude response tends to drive the servo unstable and make wideband servo control rather difficult.

The two remaining modes near 10 and 14 Hz are important in that they will degrade the disturbance rejection ability of the system. By themselves however, these two modes do not have any strong implications for the servo crossover frequency. From the standpoint of the dynamic stability of the closed loop servo system, the crossover frequency could be higher than either of these two frequencies.

Considering now the implications of the locked rotor, locked encoder, and free boundary modes, it is fair to start by dismissing the locked rotor modes as unimportant in this system. The lowest locked rotor frequency does not appear in the servo system, and the higher frequency is only coincidentally near a frequency of significance.

With knowledge of the mode shapes, the locked encoder modes will yield useful information about the system. This is especially true in the specific case of telescope design with its particular distribution of inertias and compliances. First, the mode shape which involves k_t (the 10 Hz mode) is an indicator of the disturbance rejection capability of the final system. Since the magnitude response drops (as shown in Figure 2), there will be less feedback, and the servo will be less able to reject disturbances at that frequency.

The locked encoder mode near 250 Hz which involves k_d is a good indicator of the obtainable servo crossover frequency. Note that this frequency is the frequency of resonance of the motor rotor with the drive compliance when the drive output is grounded. Considered rigorously, this frequency is only an approximation of the frequency of importance which shows up as a free boundary mode slightly higher than 250 Hz. Nevertheless, in the case of a reasonable telescope design, this approximation will be very good and slightly conservative.

In the absence of a frequency response, the free boundary modes give the most reliable indicator of the obtainable servo crossover frequency and a moderately good indication of the disturbance rejection capability of the final system. First, by identifying the mode in which there is a large phase lag between the point where the controlled input is applied (torque at the motor rotor) and the output is taken (position of the load), the crossover limiting frequency can be found. In this instance, this is again the mode near 250 Hz.

Next, the free boundary frequencies lower than this limiting frequency will give some indication of the disturbance rejection degradation of the final system. For every free boundary mode lower than the crossover limiting frequency, there will be a preceding antiresonance with a resulting disturbance rejection degradation.

CONCLUSIONS

The influence of the various vibrational modes is best found from a frequequency response with the proper variables as inputs and outputs.

In general, the lowest frequency mode in a frequency response does not limit the obtainable servo crossover frequency. The crossover frequency will be limited by the first mode which introduces a large phase lag between the point where the servo input is applied and the output is measured. Still, any modes at frequencies lower than this mode will degrade the disturbance rejection capability of the system at those frequencies.

With proper interpretation, the free boundary modes can indicate which modes degrade disturbance rejection and which mode limits the servo crossover frequency. The locked encoder modes can also approximate this information with sufficient accuracy when the drive inertia and stiffness are small compared to the inertia and stiffness of the driven load. This is the case for any reasonable large telescope design.

Locked rotor modes should not be used in evaluating the performance of a system where torque is applied on one side of the drive compliance and position is encoded on the other side.

APPENDIX A

Frequency Response Derivation

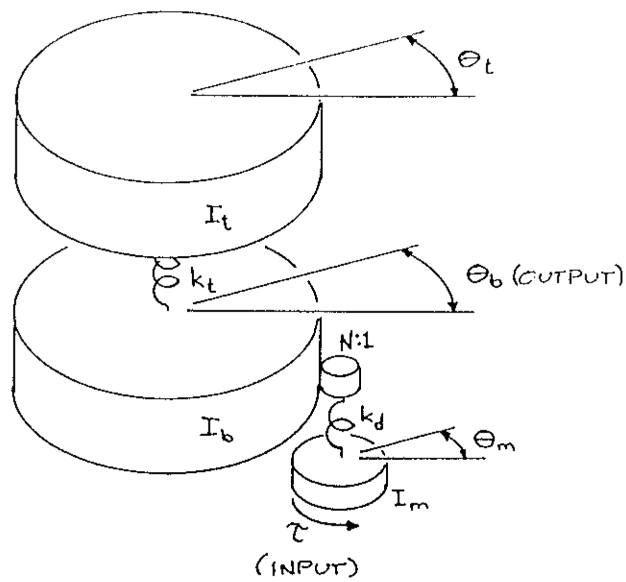

The equations of motion for this system are

$$k_t(\Theta_b-\Theta_t)-I_t\ddot{\Theta}_t=0$$

$$k_t(\Theta_t-\Theta_b)+k_d(N\Theta_m-N^2\Theta_b)-I_b\ddot{\Theta}_b=0$$

$$k_d(N\Theta_b-\Theta_m)-I_m\ddot{\Theta}_m+\tau=0$$

Taking the Laplace transform and combining the equations of motion yeilds

$$\frac{\Theta_b}{\mathrm{T}}=\frac{Nkd(I_t s^2+k_t)}{s^2[I_m I_b I_t S^4+(k_d I_t(I_b+N^2 I_m)+k_t I_m(I_b+I_t))s^2+k_d k_t(N^2 I_m+I_b+I_t)]}$$

Where Θ_b and T are the transformed time functions θ_b and T, and s is the transform variable. This transfer function shows zeros (zeros of the numerator) at

$$s=\pm j\sqrt{\frac{k_t}{I_t}}$$

and poles (zero of the denominator) at

$$s=0,\,0,\,\pm\left(\frac{-b\pm\sqrt{b^2-4ac}}{2a}\right)^{\frac{1}{2}}$$

where

$$a=I_m I_b I_t$$

$$b=k_d I_t\,(I_b+N^2 I_m)+k_t I_m\,(I_b+I_t)$$

$$c=k_d k_t\,(N^2 I_m+I_b+I_t)$$

The magnitude response of this system is

$$\left|\frac{\Theta_b}{\mathrm{T}}\right|=\left[\left(\frac{\Theta_b}{\mathrm{T}}\right)\left(\frac{\Theta_b}{\mathrm{T}}\right)^*\right]^{\frac{1}{2}}_{s=2\pi jf}$$

where the asterisk denotes the complex conjugate. The phase response of this system is

$$ARG\left(\frac{\Theta_b}{\mathrm{T}}\right)_{s=2\pi jf}$$

APPENDIX B

Mode Frequencies for Various Boundary Conditions

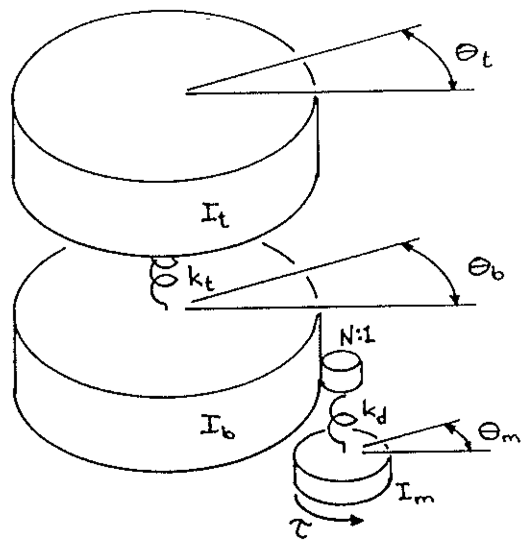

Free Boundary Frequencies:
The frequencies of the free boundary modes of vibration are simply the poles of the transfer function found in Appendix A. Repeated here, the roots are

$$s=0,0,\pm\left(\frac{-b\pm\sqrt{b^2-4ac}}{2a}\right)^{\frac{1}{2}}$$

where $s=2\pi jf$, and

$$a=I_m I_b I_t$$

$$b=k_d I_t(I_b+N^2 I_m)+k_t I_m(I_b+I_t)$$

$$c=k_d k_t(N^2 I_m+I_b+I_t)$$

Locked Encoder Frequencies:
The locked encoder condition effectively grounds I_b and removes it from the system. As a result, I_m and I_t are isolated, and the Laplace transformed equations of motion become

$$\Theta_t(k_t+I_t s^2)=0$$

$$\Theta_m(k_d+I_d s^2)=0$$

These equations have roots at

$$s=\pm j\sqrt{\frac{k_t}{I_t}},\ \pm j\sqrt{\frac{k_d}{I_d}}$$

$$\textit{where } s=2\pi jf$$

Locked Rotor Frequencies:
The locked rotor condition effectively grounds I_m and removes it from the system. The Laplace transformed equations of motion become

$$\Theta_b k_t-\Theta_t(k_t+I_t s^2)=0$$

$$\Theta_t k_t-\Theta_b(k_t+k_d+I_b s^2)=0$$

The characteristic equation (determinant) for this system is

$$I_t I_b s^4+(k_t(I_b+I_t)+k_d I_t)s^2+k_d k_t=0$$

which has its roots at

$$s=\pm\left(\frac{-b\pm\sqrt{b^2-4ac}}{2a}\right)^{\frac{1}{2}}$$

where

$$s=2\pi jf$$

$$a=I_t I_b$$

$$b = (k_t(I_b + I_t) + k_d I_t)$$

$$c = k_d k_t$$

APPENDIX C

Plot Generating Program

```
% This file runs in Matlab.
% Calculates the dynamic response of a three-inertia, two-spring system.
% Intended to simulate the first flexible mode of a driven load, and the
% first important compliance of the drive mechanism.  For the transfer
% function, torque is applied to Im and output position is taken at Ib.

N=40; %Drive ratio
Ia=4e6;
Ib=Ia/2;          %Bottom inertia.
It=Ia/2;          %Top inertia.
Im=1;             %Motor inertia.
ftle=10;          %Locked encoder frequency (It on kt).
fdls=250;         %Locked encoder frequency (Im on kd).
kt=(2*pi*ftle)^2 * It;
kd=(2*pi*fdls)^2 * Im;

num=(N*kd)*[It 0 kt]; %Numerator polynomial.
den=[(Im*Ib*It) 0 ((kd*It*(Ib+(N^2*Im)) + (kt*Im)*(Ib+It)) ...
    0 (kd*kt)*((N^2*Im)+Ib+It) 0 0]; %Denominator polynomial.

[zeros,poles,k]=tf2zp(num,den); %Solve for zeros, poles, and gain of system.
zeros=roots(num);
poles=roots(den);

poles=poles - (0.01*sqrt(conj(poles).*poles)); %Add some damping.
zeros=zeros - (0.01*sqrt(conj(zeros).*zeros));

f=logspace(0,3,500);
[dnum,dden]=zp2tf(zeros,poles,k); %Form damped transfer function.
[mag,phase]=bode(dnum,dden,2*pi*f); %Calculate frequency response.

loglog(f,mag),grid %Generate the plots.
title('Magnitude vs. Frequency (torque input, base position output)')
xlabel('Frequency (Hz)')
ylabel('Magnitude (rad/Nm)')
pause

A=input('Save the plot? Y/N [N]:','s');
if isempty(A)
        A='N';
end

if A~='N'
        meta d:\matlab\wiyn\threebdplot
end

semilogx(f,phase+180),grid
title('Phase vs. Frequency (torque input, base position output)')
xlabel('Frequency (Hz)')
ylabel('Phase (degrees)')

pause

A=input('Save the plot? Y/N [N]:','s');
if isempty(A)
        A='N';
end

if A~='N'
        meta d:\matlab\wiyn\threebdplot

end

%Find the locked rotor roots.
lrroots=roots([ It*Ib 0 (kt*Ib+kt*It+kd*It) 0 kd*kt ]);
```